PROCEEDINGS OF SCIENCE

# Exotic hadrons: review and perspective

**Qian Wang**[a,b,c,*]

[a] *State Key Laboratory of Nuclear Physics and Technology, Institute of Quantum Matter, South China Normal University, Guangzhou 510006, China*

[b] *Research Center for Nuclear Physics (RCNP), Osaka University, Ibaraki 567-0047, Japan*

[c] *Southern Center for Nuclear-Science Theory (SCNT), Institute of Modern Physics, Chinese Academy of Sciences, Huizhou 516000, Guangdong Province, China*

*E-mail:* qianwang@m.scnu.edu.cn

This proceeding reviews exotic hadron studies presented at Hadron 2025, focusing on competing interpretations of the $\chi_{c1}(3872)$ (hybrid, the $D\bar{D}^*$ molecule, the mixture between the $D\bar{D}^*$ molecule and conventional charmonium) and $T_{cc}^+$ (the $DD^*$ molecule, compact tetraquark, hybrid). Their properties are examined via lattice QCD, effective theories, and experimental constraints. Emerging directions include many-hadron systems, finite-temperature behavior, and machine learning approach. Those are important complementary approaches to decipher the internal exotic hadrons.

*The 21st International Conference on Hadron Spectroscopy and Structure (HADRON2025)*
*27 - 31 March, 2025*
*Osaka University, Japan*

*Speaker

 ISSN 1824-8039 . Published by SISSA Medialab.



PoS(HADRON2025)190

## 1. Introduction

Hadron properties provide a crucial platform for understanding the strong force, with significant cross-disciplinary relevance. For example, protons and neutrons, as the building blocks of nuclei, rely on hadronic interactions to explain nuclear binding mechanisms. The Hadron 2025 conference reflects this breadth, featuring topics such as: 1) Meson and baryon spectroscopy, 2) Exotic hadrons and candidates, 3) Hadron decays, production, and interactions, 4) Structure functions, 5) Hadrons in hot/dense media Nuclei with strange, charm, and bottom flavors 6) Beyond-Standard-Model physics 7) Theoretical methods, analysis tools, instruments, and facilities. While this talk focuses on exotic hadrons and candidates, which inherently connects to other themes. For instance, hadron interactions determine whether multi-hadron systems can form hadronic molecules. With increasing experimental statistics, dozens of exotic candidates have emerged [1–3], interpretable as hadronic molecules, compact multiquark states, kinematic effects, or other configurations.

Methodologically, traditional approaches, including quark models, QCD sum rules, effective field theories, and lattice QCD, are employed to probe their nature. New techniques further increase the calculation precision, such as the complex scaling method for determining the resonance pole. Studies of hadrons in nuclear matter and at finite temperature also attract intense interest, contrasting their vacuum properties. Advances in computational science are accelerating progress, notably through machine learning applications within the hadron physics community.

Since Hadron 2023, significant progress has been made in the hadron community, particularly regarding exotic candidates such as: 1) charmonium-like states $\chi_{c1}(3872)$, $P_c$, $P_{c\bar{c}s\bar{s}}$, $P_{c\bar{c}s}$ states. 2) open-charm/double charm system $T_{cc}^+$, $D_{s0}(2317)$, $D_0^*(2300)$. 3) strange/bottom hyperons $\Lambda(1405)$, $\Omega(2012)$. 4) light-quark exotics $\Theta^+$, $a_0/f_0(980)$, $\phi(2170)$, light hybrids, and glueballs. 5) four different flavors $bc\bar{s}\bar{q}$ and fully charm state $X(6200)$. All advances for these states were reported at Hadron 2025, with particular interest focused on $\chi_{c1}(3872)$, and $T_{cc}^+$ states. In subsequent sections, I would review the progress of these two states presented at Hadron 2025 conference, and present my personal perspectives for interesting topics to understand hadron properties. Before that, I do apologize for any relevant works not included in this proceeding, which summarizes conference talks exclusively. In the following, I will compare related presentations and propose experimentally distinguishable observables to test competing theoretical scenarios.

## 2. Review of exotic candidates reported at Hadron 2025

There are several talks on exotic candidates at Hadron 2025. Most of them focus on the $\chi_{c1}(3872)$ and $T_{cc}^+$. In the following, I would compare the presentations about their natures in this conference and propose potential experimental distinguishable observables.

### 2.1 $\chi_{c1}(3872)$

The $\chi_{c1}(3872)$, also known as $X(3872)$, is the first exotic candidate and has been intensively studied. Three competitive scenarios are presented at this conference, i.e. the hybrid state, the $D\bar{D}^*$ hadronic molecule, and a mixture between the $D\bar{D}^*$ hadronic molecule and the conventional $c\bar{c}$ charmonium. While all three can explain the observed mass, they make distinct predictions which can be used to distinguish between them.

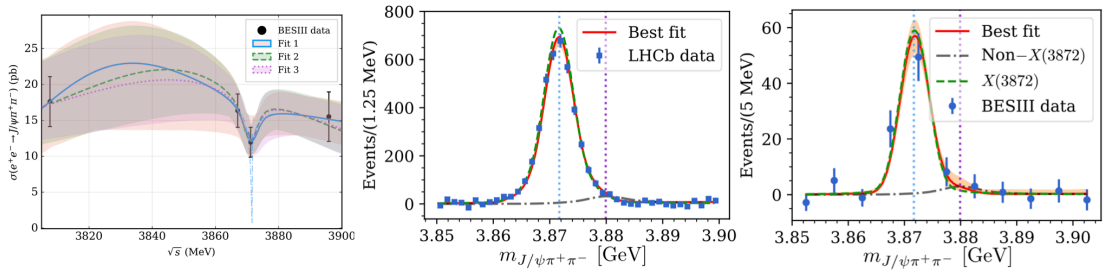


**Figure 1:** The left figure is from Ref. [6] for the $e^+e^- \to J/\psi\pi^+\pi^-$ process. The signal behaves as a dip structure as it is driven by the $J/\psi\rho$ channel. The middle and right figures are from Ref. [7] for the $B^+ \to K^+J/\psi\pi^+\pi^-$ and $e^+e^- \to \gamma J/\psi\pi^+\pi^-$ processes, respectively. Those structures are driven by the $D\bar{D}^*$ channels, expressing themselves as peak structures.

The $\chi_{c1}(3872)$ is interpreted as a hybrid state in a model, where its mass is obtained by solving the Schrödinger equation [4] using a potential for the light degrees of freedom derived from lattice QCD. This approach employs the Born-Oppenheimer Effective Field Theory (BOEFT) approach, which treats heavy quarks as moving adiabatically in the presence of the light degrees of freedom. The model yields probabilities of $8-13\%$ for $\Sigma_g^+$, $38\%$ for $\Sigma_g^{+\prime}$, and $54\%$ for $\Pi_g$. The resulting hybrid multiplet spectrum [4] contains one $1^{+-}$ state at 3957 MeV, one $0^{++}$ state at 3846 MeV and one $2^{++}$ state at 4004 MeV. The $1^{+-}$ state may correspond to the $X(3940)$ observed by Belle collaboration. This spectrum is significantly different from that in the molecular picture, i.e. Fig.2 of Ref. [5], which predicts two $0^{++}$ states, two $1^{+-}$ states, one $1^{++}$ and one $2^{++}$ states. Notably, the lower $0^{++}$ and higher $1^{+-}$ masses in the molecular picture are similar to those in the BOEFT method. Discriminating between these scenarios requires searching for the higher $0^{++}$ state near the $D^*\bar{D}^*$ threshold and the lower $1^{+-}$ state near the $D\bar{D}^*$ threshold. Importantly, the observed $\chi_{c1}(3872)$ has a radius of 15 fm, characteristic of a hadronic molecule. The predicted branching ratio fraction [4]

$$\frac{\Gamma(\chi_{c1}(3872) \to \gamma\psi(2S))}{\Gamma(\chi_{c1}(3872) \to \gamma J/\psi)} = 2.99 \pm 2.36 \tag{1}$$

is in agreement with the LHCb measurement $1.67 \pm 0.25$ within the uncertainty. However, the theoretical uncertainties remain substantial and require further reduction.

Due to its mass very close to the $D\bar{D}^*$ threshold, the $\chi_{c1}(3872)$ could be the $D\bar{D}^*$ hadronic molecule, or that with a mixture of $c\bar{c}$ charmonium state. These two scenarios are also presented at Hadron 2025. The property of the $\chi_{c1}(3872)$ is precisely determined from the $e^+e^- \to \gamma(D^0\bar{D}^{*0}\pi^0)/\gamma(J/\psi\pi^+\pi^-)$ and $B^+ \to K^+(J/\psi\pi^+\pi^-)$ data. The $D\bar{D}^*$ and $J/\psi\pi^+\pi^-$ channels are considered as the elastic and inelastic channels, respectively. The extracted pole position is $E_X = (-53^{+10}_{-25} - i34^{+2}_{-12})$ MeV [7] and its isospin partner, named as $W^0_{c1}$, is also predicted with pole position $E_W = (1.6^{+0.7}_{-0.9} + i1.4^{+0.3}_{-0.6})$ MeV [7]. The compositeness is $\bar{X}_A = \left(1 + 2\left|\frac{\mathrm{Re}\, r_0 - \Delta r_{0,IIB}}{\mathrm{Re}\, a_0}\right|\right)^{-\frac{1}{2}} > 0.99$ with $r_0$, $a_0$ the effective range and scattering length, respectively. The compositeness value indicates that the $\chi_{c1}(3872)$ has a large probability to be a hadronic molecular state. $r_{0,IIB}$ is the effective range with corrections from isospin breaking. In contrast, whether the BOEFT approach can encode isospin information depends on the BO potential extracted from lattice QCD. Whether the $\chi_{c1}(3872)$ behaves as a peak or a dip depends on the driven product vertex. It behaves as a dip structure in the $e^+e^- \to J/\psi\pi^+\pi^-$ [6] process and a peak structure in the $e^+e^- \to \gamma J/\psi\pi^+\pi^-$,

$B^+ \to K^+ J/\psi\pi^+\pi^-$ [7] process, as shown by Fig. 1. The reason is that the former one is driven by the $J/\psi\rho$ channel and the latter one is driven by the $D\bar{D}^*$ channels. This is the unique feature in hardonic molecular picture, whose signals behave differently in various channels. When a mixture of the $c\bar{c}$ charmonium is considered in the molecular picture, the compositeness can vary from 0 to 1 [8]

$$X = \left[1 + \frac{g_0^2 \kappa\mu(\kappa+\mu)^3}{8\pi m^2 \left(g_0^2 + (E-E_0)\,\omega^h\right)^2}\right]^{-1} = \left[1 + 2\pi \frac{g_0^2}{(B+E_0)^2} \frac{\kappa}{\mu(\mu+\kappa)}\right]^{-1} \tag{2}$$

which corresponds to the elementary and molecular pictures, respectively. Here $E_0$ and $E$ are the energy of the bare state and the energy of the system. $m$ is the mass of the interacted particle and $\mu$ is their reduced mass. This compositeness can also be reflected in the values of the scattering length and effective range. For a pure molecule [9], the scattering length and effective range are

$$a = -2\left(\frac{1-\lambda^2}{2-\lambda^2}\right)\frac{1}{\gamma}, \quad r = -\left(\frac{\lambda^2}{1-\lambda^2}\right)\frac{1}{\gamma}. \tag{3}$$

Here $\lambda^2$ is the probability to find the compact component of the wave function in the physical state. $\gamma$ is the binding momentum. For a pure near-threshold hadronic molecule, i.e. $\lambda^2 = 0$, the scattering length is very large and the effective range is very small, making the compositeness almost 1. When the elementary object is considered, the scattering length and effective range read as [10]

$$1/a = \frac{g_i}{M_{\rm CDD} - M_{\rm th}} - \beta, \quad r = -\frac{g_i}{\mu\,(M_{\rm th} - M_{\rm CDD})^2}, \tag{4}$$

where $M_{\rm th}$ and $M_{\rm CDD}$ (corresponding to the zero of the T-matrix element) are the positions of the threshold and the CDD pole. $\beta$ is the range of the force. When $M_{\rm CDD}$ is far away from $M_{\rm th}$, the modulus $r$ is about 1 fm. Otherwise, $r$ is a very large value. Whether the CDD pole approaches the threshold is determined by the experimental data. If the data do not require a near-threshold CDD pole, it will almost come back to pure hadronic molecular case.

The Coulomb force, as an infinity long-range force, is very important for near-threshold states. For instance, the inclusion of Coulomb force changes the bound $\Omega_{ccc}\Omega_{ccc}$ system to a resonance [11]. One can also see that a repulsive Coulomb force makes a bound state pole directly to a resonance [12], and the Coulomb scattering length moves from a positive value to a negative value simultaneously. The compositeness behavior also depends on the strength of the Coulomb force. As this Coulomb force stems from the photon exchanged diagram, which is related to the lineshape of the $\chi_{c1}(3872)$ in the $\gamma D\bar{D}$ channel. A detailed study from both theoretical side and experimental side is very important for the role of Coulomb force in the formation of the $\chi_{c1}(3872)$.

The hidden charm decay channel $J/\psi\pi^+\pi^-$ is the first measured channel of the $\chi_{c1}(3872)$ and very important for its internal structure. The decay is dominantly via the quark interchanged mechanism of its $D\bar{D}^*$ component [13]. The predicted branching ratio fraction is

$$\frac{\mathcal{B}(\chi_{c1}(3872) \to J/\psi\pi^+\pi^-\pi^0)}{\mathcal{B}(\chi_{c1}(3872) \to J/\psi\pi^+\pi^-)} = 1.8 \tag{5}$$

which agrees with the value $1.0 \pm 0.4 \pm 0.3$ from Belle collaboration. As the two pions are from the $\rho$ meson, it is an isospin breaking decay mode. This large isospin breaking effect is an unique feature of hadronic molecular state.

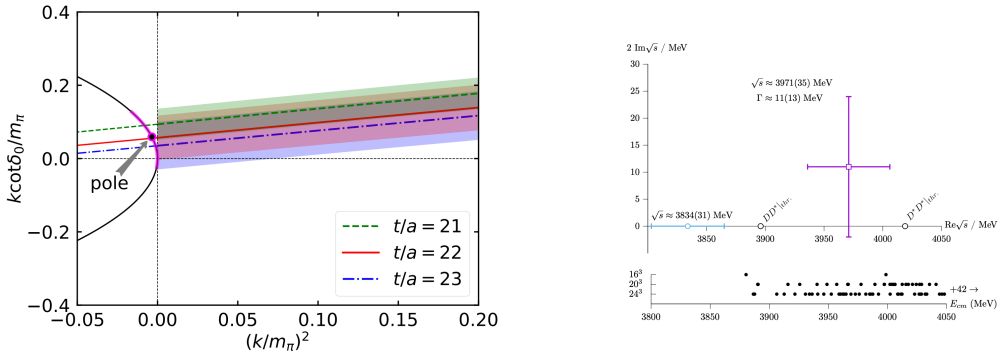


**Figure 2:** The left figure is from Ref. [19]. It shows the $k \cot \delta_0/m_\pi$ for the $DD^*$ scattering in the $I = 0$ and $S$-wave channel as a function of $(k/m_\pi)^2$. The right figure is from Ref. [20], which shows the virtual state (light blue circle) and resonance (purple box).

### 2.2 $T_{cc}$

Three competing pictures describe the double charm tetraquark $T_{cc}$, i.e. the $DD^*$ hadronic molecule, the compact $cc\bar{q}\bar{q}$ tetraquark, and the hybrid state within the Born-Oppenheimer (BO) potential. In the BOEFT approach, the $T_{cc}^+$ corresponds to the lower $J^P = 1^+$ isospin singlet state [4], characterized by orbital angular momentum $l = 0$ and heavy-quark spin $S_Q = 1$. This configuration yields a spatial extent of $\sim 8$ fm, characteristic of hadronic molecules. The same multiplet contains additional two $1^-$, one $0^-$, one $0^+$ and one $2^+$ states.

The primary motivation for interpreting the $T_{cc}^+$ as a $DD^*$ hadronic molecule stems from its proximity to the $DD^*$ threshold. Research in this framework follows two main approaches. One involves solving integral equations, either Lippmann-Schwinger equation or Bethe-Salpeter equation, to obtain the scattering amplitudes and extract dynamical parameters directly from experimental data [14–18]. The other involves computing the $DD^*$ scattering amplitudes via the lattice [19–24] simulations. In the first approach, various studies differ primarily in their treatment of $DD^*$ interactions. Ref. [14] implements three forms of interactions, i.e. only contact potentials with static $D^*$ width, contact potentials with incomplete 3-body unitarity, One-Pion-Exchanged (OPE) potential and full 3-body unitarity. All of them can describe the experimental data very well. The full 3-body unitarity yields a pole position at $-356^{+39}_{-38} - i(28 \pm 1)$ keV. Complementary analyses give effective ranges of $-2.4 \pm 0.01 \pm 0.85$ fm without isospin breaking and $1.38 \pm 0.01 \pm 0.85$ fm with isospin breaking [25]. This resolves the doubts regarding the $T_{cc}^+$ as a $DD^*$ hadronic molecular state.

Ref. [15] constructs the $DD^*$ interaction using hidden local gauge symmetry, which successfully explains the lineshape in the $DD\pi$ channel [16], consistent with the physical poles being constrained by the experimental data. Ref. [16] further establishes the $T_{cc}^+$ as a molecular state with $(100 \pm 3)\%$ molecular probability. Through inverse-problem analysis of the $D^0D^+$ and $D^+D^0$ channel interactions, they confirm the $T_{cc}^+$ has isospin $I = 0$ and molecular composition: $P_{D^0D^{*+}} = 70\%$ and $P_{D^+D^{*0}} = 30\%$. One can also construct the $DD^*$ interaction via One-Boson-Exchanged Potential (OBEP) and also give the correct $T_{cc}^+$ mass position [18, 26].

All the aforementioned approaches rely on non-relativistic approximations, relativistic correc-

tions become significant at energies far from the $DD^*$ threshold. Ref. [17] addresses this through a relativistic analysis of the $T_{cc}^+$ lineshape in the $D^0D^0\pi^+$ channels. Both considered schemes, i.e. pure contact interactions, and contact interactions plus One-Pion-Exchange (OPE) potential, successfully describe the data. For the later case, the extracted $T_{cc}^+$ pole position is $-351^{+37}_{-35} - i(28 \pm 1)$ keV, consistent with that in Ref. [14] within the uncertainties. This agreement is expected since the pole's proximity to the $DD^*$ threshold implies minimal relativistic corrections.

A study [18] examining both the hadronic molecule and a mixed scenario with the compact tetrquark components reveals that the current experimental data supports multiple interpretations. While the lineshape fails to distinguish between these models, further measurements could resolve their compatibility. The compact tetraquark model describes hadrons bound primarily through the color force. In this framework, the $T_{cc}^+$ is interpreted as an isospin singlet $J^P = 1^+$ tetraquark within the diquark-antidiquark picture [27]. However, this approach predicts numerous partner states beyond typical expectations. As emphasized by Jean-Marc Richard, rigorous spectrum of multiquark states must include all the possible configurations. Any truncated bases fail to produce reliable mass spectra.

The lattice QCD can determine whether a $DD^*$ hadronic molecular state exists by calculating $DD^*$ scattering. HALQCD Collaboration [19] perform simulations at several pion masses near the physical value. At $m_\pi = 146.4$ MeV, their results show that the $T_{cc}^+$ behaves as a near-threshold virtual state, with its pole position well above the left-hand cut [28] (left figure of Fig. 2). The extracted scattering length agrees remarkably well with the LHCb data. Cruicially, when extrapolated to the physical pion mass, this virtual state becomes a bound state. A study by Whyte et al. [20] investigates $DD^* - D^*D^*$ scattering at heavier pion mass $m_\pi = 391$ MeV and finds a virtual state below the $DD^*$ threshold (right figure of Fig. 2). However, as the $D$ and $D^*$ meson masses are 1886 MeV and 2010 MeV, respectively, in their simulation, the corresponding three momentum square $p^2 = 2\mu_{DD^*}(E - m_D - m_{D^*}) = -120654$ MeV$^2$ is significantly below the estimated left-hand cut $p^2_{\rm lhc} = \frac{1}{4}((m^*_{D^*} - m_D)^2 - m^2_\pi) = --34181$ MeV$^2$. This raises questions about the reliability of the pole position below left-hand cut extracted at his unphysical pion mass, which remains under discussion. Additional lattice QCD results concerning the $T_{cc}^+$ exist [21–24], though they were not presented at this conference.

## 3. Perspective

This conference has brought us methodological and technical innovations, as we attempt to use machine learning to study hadron properties. Our focus has also expanded from two-hadron systems to multi-hadron systems. The increasing statistical data in heavy-ion collisions makes it possible to study the properties of exotic candidates at finite temperature and nuclear matter. From my point of view, these advances may open a new window for understanding the nature of hadrons.

### 3.1 Many-hadron systems

The deuteron (a bound state of a proton and a neutron) demonstrates how two-nucleon systems can form stable states. Similarly, many-nucleon systems could form stable nuclei. Analogously, if the two-hadron molecules exist, many-hadron systems may also exhibit significant formation probabilities for stable configurations. Current research in this domain includes contributions

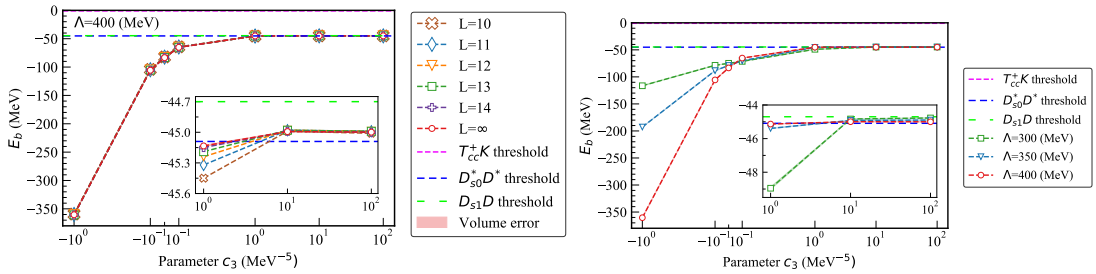


**Figure 3:** The figures are from Ref. [29]. The left figure is the three-body binding energy in terms of the three-body interaction parameter $c_3$. The orange crosses, blue diamonds, yellow inverted triangles, green squares, and purple plus are for volume $L = 10, 11, 12, 13, 14$ in order. The red circles and bounds are the central value and uncertainty when $L \to \infty$ by using the extrapolation formula $\frac{\Delta E}{E_T} = -(\kappa L)^{-3/2} \sum_{i=1}^{3} C_i \exp(-\mu_i \kappa L)$. The right figure is the three-body binding energy at infinity volume for the lattice cutoff parameter $\Lambda = 300$ MeV (green squares), 350 MeV (blue inverted triangles), 400 MeV (red circles).

from E. Oset, T. Hyodo, K.P. Khemchandani, A.Martinez Torres, L.S.Geng, C.W. Xiao, M.P. Valderramma, A. Hosaka, F.K.Guo and so on, with comprehensive reviews on three-hadron systems available in Refs. [30, 31]. At this conference, Hailong Fu presented results on the Efimov effect [32] in the $D^*D^*D^*$ system. They conclude that whether the Efimov effect exists or not depends on the isospin triplet interactions. However, as the $D^*$ meson is unstable, experimental detection of such three-body bound states is fundamentally unfeasible. Instead, the three $D$ system offers a viable alternative since the $D$ meson is stable under strong interaction [1]. Our recent work [29] investigates the $DD^*K$ system on the lattice, incorporating direct three-body interactions. The two-body sub-interactions are well-constrained by experimental data on $T_{cc}^+$, $D_{s0}(2317)$, and $D_{s1}(2460)$. Figure 3 demonstrates that a three-body bound state persists regardless of the strength of the direct three-body interaction.

### 3.2 Hadron properties at finite temperature and nucleon density

From the first exotic signature detected in Heavy Ion Collisions (HIC) [34], properties of hadrons at finite temperature and nuclear matter have served as vital complementary probes to decipher their internal configurations. Properties of hadrons produced in HIC could be different from that in vacuum, as its property could be affected by finite temperature and nucleon density. For instance, the $DD^*$ scattering amplitudes significantly depend on the nuclear density [33]. When the nuclear density increases, the near-threshold structure becomes broader. In addition, the behavior of $\bar{D}\bar{D}^*$ scattering amplitude is different from the $DD^*$ scattering amplitude, which indicates that particles and antiparticles have different behaviors in nuclear matter [33].

The study of exotic candidates at finite temperature and nuclear matter offers a potential advantage: distinguishing between different theoretical scenarios. We have tested this approach for the $Z_c(3900)$ by comparing its $D\bar{D}^*$ hadronic molecular interpretation with the triangle singularity mechanism [35]. Both scenarios successfully reproduce experimental vacuum data. However, as temperature increases, their spectral peaks exhibit similar modifications, i.e. shifting toward lower

[1] Comments from Eulogio Oset.

energies and broadening. To resolve this ambiguity, the distinct temperature-dependent trajectories of the pole position (molecular scenario) and triangle singularity can provide critical discrimination.

### 3.3 Machine learning approach

While machine learning (ML) techniques from computer science show great potential for solving difficult physics problems, their conclusions often remain tied to the input models. This is illustrated by Refs. [38], which apply neural networks to classify the $P_c(4312)$ (e.g., as a triangle singularity, rescattering effect, or genuine resonance). Ref. [38], extending Ref. [39], finds the state consistent with a genuine resonance resulting from $J/\psi p$-$\Sigma_c \bar{D}$ rescattering. Yet, both results are inherently model-dependent, as they rely on specific theoretical assumptions to generate the training samples.

To address the issue of model dependence, the research subject investigated using neural networks should be distinguished from the theory used to generate the training set. For instance, Ref. [37] employs Lattice Effective Field Theory (EFT) to compute finite-volume energy shifts for both short- and long-range interactions. These shifts are processed via symbolic regression to derive an extrapolation formula, critical for Lattice calculations. The study reveals a universal exponential scaling law for the energy shift $E_L = C_1 + C_2 e^{-C_3 L} L^n$ applicable both short- and long- range interactions. This demonstrates a model-independent approach to integrating machine learning in theoretical physics.

## 4. Summary and outlook

Hadrons, particularly exotic hadrons, provide a valuable platform for studying the non-perturbative regime of strong interactions. While traditional methods have successfully characterized some of their properties, persisting challenges necessitate novel approaches for further investigation, for instance, many-body systems, the properties of hadrons at finite temperature and nuclear matter, machine learning approach and so on.

## References

[1] S. L. Olsen, T. Skwarnicki and D. Zieminska, Rev. Mod. Phys. **90**, no.1, 015003 (2018) [arXiv:1708.04012 [hep-ph]].

[2] C. Z. Yuan, Natl. Sci. Rev. **8**, no.11, nwab182 (2021) [arXiv:2102.12044 [hep-ex]].

[3] N. Brambilla, S. Eidelman, C. Hanhart, A. Nefediev, C. P. Shen, C. E. Thomas, A. Vairo and C. Z. Yuan, Phys. Rept. **873**, 1-154 (2020) [arXiv:1907.07583 [hep-ex]].

[4] N. Brambilla, A. Mohapatra, T. Scirpa and A. Vairo, [arXiv:2411.14306 [hep-ph]].

[5] X. K. Dong, F. K. Guo and B. S. Zou, Progr. Phys. **41**, 65-93 (2021) [arXiv:2101.01021 [hep-ph]].

[6] V. Baru, F. K. Guo, C. Hanhart and A. Nefediev, Phys. Rev. D **109**, no.11, L111501 (2024) [arXiv:2404.12003 [hep-ph]].

[7] T. Ji, X. K. Dong, F. K. Guo, C. Hanhart and U.-G. Meißner, [arXiv:2502.04458 [hep-ph]].

[8] I. Terashima and T. Hyodo, Phys. Rev. C **108**, no.3, 035204 (2023) [arXiv:2305.10689 [hep-ph]].

[9] F. K. Guo, C. Hanhart, U. G. Meißner, Q. Wang, Q. Zhao and B. S. Zou, Rev. Mod. Phys. **90**, no.1, 015004 (2018) [erratum: Rev. Mod. Phys. **94**, no.2, 029901 (2022)] [arXiv:1705.00141 [hep-ph]].

[10] X. W. Kang and J. A. Oller, Eur. Phys. J. C **77**, no.6, 399 (2017) [arXiv:1612.08420 [hep-ph]].

[11] Y. Lyu, H. Tong, T. Sugiura, S. Aoki, T. Doi, T. Hatsuda, J. Meng and T. Miyamoto, Phys. Rev. Lett. **127**, no.7, 072003 (2021) [arXiv:2102.00181 [hep-lat]].

[12] T. Kinugawa and T. Hyodo, Eur. Phys. J. A **61**, no.7, 154 (2025) [arXiv:2411.12285 [hep-ph]].

[13] G. J. Wang, Z. Yang, J. J. Wu, M. Oka and S. L. Zhu, Sci. Bull. **69**, 3036-3041 (2024) [arXiv:2306.12406 [hep-ph]].

[14] M. L. Du, V. Baru, X. K. Dong, A. Filin, F. K. Guo, C. Hanhart, A. Nefediev, J. Nieves and Q. Wang, Phys. Rev. D **105**, no.1, 014024 (2022) [arXiv:2110.13765 [hep-ph]].

[15] A. Feijoo, W. H. Liang and E. Oset, Phys. Rev. D **104**, no.11, 114015 (2021) [arXiv:2108.02730 [hep-ph]].

[16] L. R. Dai, L. M. Abreu, A. Feijoo and E. Oset, Eur. Phys. J. C **83**, no.10, 983 (2023) [arXiv:2304.01870 [hep-ph]].

[17] X. Zhang, Phys. Rev. D **109**, no.9, 094010 (2024) [arXiv:2402.02151 [hep-ph]].

[18] M. Sakai and Y. Yamaguchi, Phys. Rev. D **109**, no.5, 054016 (2024) [arXiv:2312.08663 [hep-ph]].

[19] Y. Lyu, S. Aoki, T. Doi, T. Hatsuda, Y. Ikeda and J. Meng, Phys. Rev. Lett. **131**, no.16, 161901 (2023) [arXiv:2302.04505 [hep-lat]].

[20] T. Whyte *et al.* [Hadron Spectrum], Phys. Rev. D **111**, no.3, 034511 (2025) [arXiv:2405.15741 [hep-lat]].

[21] M. Padmanath and S. Prelovsek, Phys. Rev. Lett. **129**, no.3, 032002 (2022) [arXiv:2202.10110 [hep-lat]].

[22] S. Chen, C. Shi, Y. Chen, M. Gong, Z. Liu, W. Sun and R. Zhang, Phys. Lett. B **833**, 137391 (2022) [arXiv:2206.06185 [hep-lat]].

[23] S. Collins, A. Nefediev, M. Padmanath and S. Prelovsek, Phys. Rev. D **109**, no.9, 9 (2024) [arXiv:2402.14715 [hep-lat]].

[24] L. Meng, E. Ortiz-Pacheco, V. Baru, E. Epelbaum, M. Padmanath and S. Prelovsek, Phys. Rev. D **111**, no.3, 3 (2025) [arXiv:2411.06266 [hep-lat]].

[25] V. Baru, X. K. Dong, M. L. Du, A. Filin, F. K. Guo, C. Hanhart, A. Nefediev, J. Nieves and Q. Wang, Phys. Lett. B **833**, 137290 (2022) [arXiv:2110.07484 [hep-ph]].

[26] M. Sakai and Y. Yamaguchi, [arXiv:2503.11134 [hep-ph]].

[27] Y. Y. Lin, J. Y. Wang and A. Zhang, Phys. Rev. D **111**, no.1, 014015 (2025) [arXiv:2410.16902 [hep-ph]].

[28] M. L. Du, A. Filin, V. Baru, X. K. Dong, E. Epelbaum, F. K. Guo, C. Hanhart, A. Nefediev, J. Nieves and Q. Wang, Phys. Rev. Lett. **131**, no.13, 131903 (2023) [arXiv:2303.09441 [hep-ph]].

[29] Z. Zhang, X. Y. Hu, G. He, J. Liu, J. A. Shi, B. N. Lu and Q. Wang, Phys. Rev. D **111**, no.3, 036002 (2025) [arXiv:2409.01325 [hep-ph]].

[30] M. Z. Liu, Y. W. Pan, Z. W. Liu, T. W. Wu, J. X. Lu and L. S. Geng, Phys. Rept. **1108**, 1-108 (2025) [arXiv:2404.06399 [hep-ph]].

[31] T. W. Wu, Y. W. Pan, M. Z. Liu and L. S. Geng, Sci. Bull. **67**, 1735-1738 (2022) [arXiv:2208.00882 [hep-ph]].

[32] E. Braaten and H. W. Hammer, Phys. Rept. **428**, 259-390 (2006) [arXiv:cond-mat/0410417 [cond-mat]].

[33] V. Montesinos, M. Albaladejo, J. Nieves and L. Tolos, Phys. Rev. C **108**, no.3, 035205 (2023) [arXiv:2306.17673 [hep-ph]].

[34] A. M. Sirunyan *et al.* [CMS], Phys. Rev. Lett. **128**, no.3, 032001 (2022) [arXiv:2102.13048 [hep-ex]].

[35] Y. Zhang, A. Hosaka, Q. Wang and S. Yasui, Phys. Rev. D **112**, no.1, 016014 (2025) [arXiv:2503.19374 [hep-ph]].

[36] M. Ablikim *et al.* [BESIII], Phys. Rev. Lett. **110**, 252001 (2013) [arXiv:1303.5949 [hep-ex]].

[37] W. Zhang, W. J. Zhang, Z. Zhang, J. Hu, B. Lu, B. N. Lu, J. Pang, J. Y. Pang and Q. Wang, Chin. Phys. Lett. **42**, no.7, 070202 (2025) [arXiv:2503.06496 [hep-ph]].

[38] D. A. O. Co, V. A. A. Chavez and D. L. B. Sombillo, Phys. Rev. D **110**, no.11, 114034 (2024) [arXiv:2403.18265 [hep-ph]].

[39] C. Fernández-Ramírez *et al.* [JPAC], Phys. Rev. Lett. **123**, no.9, 092001 (2019) [arXiv:1904.10021 [hep-ph]].